Research article

Multi-layer encapsulation of pumpkin (*Cucurbita maxima* L.) seed protein hydrolysate and investigating its release and antioxidant activity in simulated gastrointestinal digestion

Zeinab Nooshi Manjili, Alireza Sadeghi Mahoonak [*], Mohammad Ghorbani, Hoda Shahiri Tabarestani

Department of Food Science and Technology, Gorgan University of Agricultural Sciences and Natural Resources, Gorgan, Iran

ABSTRACT

Because of their high protein content, easy access and low cost, pumpkin seeds are a valuable raw material for the preparation of antioxidant protein hydrolysates. Micro-coating is an effective method to protect bioactive compounds against destruction. In order to strengthen the alginate hydrogel network loaded with pumpkin seed protein hydrolysate (PSPH), CMC was added as part of its formulation in the first step, and chitosan coating was used in the second step. Then, swelling amount, release in the simulated gastrointestinal environment (SGI), antioxidant activity after SGI, Fourier transform infrared spectroscopy (FTIR), zeta potential, dynamic light scattering (DLS), polydispersity index (PDI) and scanning electron microscopy (SEM) of the samples were evaluated. The results showed that, the swelling amount of the chitosan-alginate hydrogel was lower than the chitosan-alginate-CMC sample, and with the increase in chitosan concentration, the swelling amount decreased. The release amount in the chitosan-alginate sample was higher than that in the chitosan-alginate-CMC sample, and with the increase in chitosan concentration, the release rate decreased. Also, the amount of release increased with the passage of time. The highest antioxidant activity belonged to the chitosan-alginate sample in SGI, and it increased with increasing the chitosan concentration. All findings demonstrated that the use of multi-component hybrid systems is a useful method for the protection of bioactive compounds against destruction, their antioxidant activities and their release behavior.

1. Introduction

Proteins are important nutritional sources for humans. These compounds provide nitrogen, amino acids and energy, which are needed for the normal function of body systems [1]. Pumpkin seeds can be used as a raw material to produce high-quality products for food formulations, as well as products with good functional properties [2]. More importantly, because of their high protein content, easy access and low cost, pumpkin seeds are valuable raw materials for the preparation of antioxidant protein hydrolysates. Pumpkin seed protein hydrolysates have high antioxidant and nitric oxide inhibitory properties and can be used as suitable ingredients in food formulations [3]. Pumpkin seed hydrolysates with suitable functional properties can be used in various food formulations to improve physical and chemical properties, increase shelf life, and act as antihypertensive and antioxidant agents in the prevention of

---

* Corresponding author.
E-mail address: sadeghiaz@gau.ac.ir (A. Sadeghi Mahoonak).

cardiovascular diseases [4].

Encapsulation is a process in which a core material (a liquid, solid or gaseous compound) is enclosed in a wall material to create capsules that are resistant to chemical and environmental interactions [5]. Micro-coating is a method to solve the problems of the physical or chemical instability of susceptible compounds. It can prevent evaporation, protect the enclosed materials from adverse environmental conditions, and reduce the sensitivity to the degradation of plant materials and their bioactive compounds [6].

Alginate is a hydrophilic carbohydrate that is extracted from various species of brown algae (*Phaeophyceae*). Alginate is a water-soluble anionic polysaccharide that has good chelation power, water retention ability, biocompatibility and biodegradability, so it is widely used as a pharmaceutical carrier. Sodium alginate is soluble in hot and cold water and creates different viscosities depending on the concentration used [7]. Sodium alginate has stiffening and gelling properties, so its ability to react with multivalent metal cations results in the formation of strong gel networks and insoluble polymers. Despite these advantages, the use of alginate also has disadvantages. For example, the porosity of alginate gel can lead to spontaneous diffusion and the loss of loaded hydrophilic compounds. Also, in the gastric-simulated environment, alginate microparticles shrink, which leads to synersis of the gel and the leakage of water-soluble substances [8]. Overall, due to its hydrophilic properties, poor emulsifying capacity, and leaking of hydrophobic compounds [9], alginate should be combined and protected with a complementary polymer to improve its encapsulation properties.

Deacetylation of the chitin polymer allows the production of chitosan, where the acetyl groups of the chitin chain are removed to form amino groups. The degree of deacetylation is directly related to the performance of chitosan in its various applications. Chitosan is a natural and non-toxic polysaccharide that is widely used due to its biocompatibility, chemical resistance and biodegradability characteristics. Chitosan is known as the second biological biopolymer in nature due to its high availability [10]. This polymer is used in the micro-encapsulation of essential oils, lipids, various foods, vitamins, drugs, vaccines, hemoglobin, microbial metabolites, etc. Chitosan has high gel-forming power; this gel is sensitive to pH changes; it changes the volume of the hydrogel; and as a result, it can be used for targeted delivery of loaded bioactive compounds [11].

Carboxymethyl cellulose (CMC) is used for pharmaceutical and biotechnological applications due to its biocompatibility and biodegradability [12]. Carboxymethyl cellulose is an anionic linear polysaccharide that is soluble in water and is used as a stabilizer and water retainer in the food and cosmetic industries [13]. Also, CMC-based hydrogels have high absorption properties but low mechanical strength; therefore, multi-component hydrogel systems can be considered to improve the mechanical strength of CMC-based hydrogels [14].

Masoomi Dezfooli, Bonnot [15] used alginate beads coated with chitosan as a probiotic delivery system in aquaculture. The high palatability and stability of chitosan-coated calcium alginate beads in seawater, along with the controlled release of live probiotics, indicate that encapsulation of probiotics in chitosan-coated beads is an efficient method for delivering probiotics in aquaculture. Alaa [16] used alginate microbeads coated with chitosan to improve the anti-inflammatory potential of Etodolac.

To the best of our knowledge, there are few studies regarding the behavior of alginate-based chitosan-coated hydrogels that contain bioactive peptides in simulated GI conditions. Therefore, the purpose of this study was to investigate the characteristics of alginate-based chitosan-coated hydrogels loaded with pumpkin protein hydrolysate in a simulated digestive environment, which includes the evaluation of swelling, release rate, and antioxidant activity of hydrolysate-loaded hydrogels. In addition, the interactions between pumpkin seed protein hydrolysates and the carriers used were investigated using Fourier transform infrared (FTIR). Finally, the zeta potential, particle size, polydispersity index of hydrogels, and surface morphology of beads were investigated by scanning electron microscopy.

2. Materials and methods

2.1. Materials

Sodium alginate, CMC, Chitosan, Calcium chloride (CaCl$_2$), Pancreatin (from porcine pancreas, 0.35 U/mg), Pepsin (from porcine gastric mucosa, 0.7 U/mg), Alcalase (2.97 U/ml), Brilliant blue, Sodium chloride (NaCl), Hydrochloric acid (HCl), Potassium dihydrogen phosphate (KH$_2$PO$_4$), Potassium bromide (KBr), Methanol, DPPH, FeCl$_2$, Ferrozine, Sulfuric acid, Sodium phosphate, and Ammonium molybdate were purchased from Sigma Aldrich and Merck.

2.2. Preparation of core materials (PSPH)

2.2.1. Production of pumpkin protein concentrate

Briefly, pumpkin fruit (*Cucurbita maxima* L.) was purchased from the local market (Astane-ashrafieh, Gilan, Iran). After separating the seeds manually, they were dried in an oven (Memmert, Germany) at 50 °C for 72 h. The dried pumpkin seeds, without peeling, were completely powdered by a mill (500 A, China) and passed through a 40-mesh sieve. Hexane was added to the powder at a ratio of 10:1 (v/w) and mixed by a shaker (Noorsanat Ferdous, Iran) at a speed of 440 rpm for 4 h. The process of oil removal continued until the remaining oil was reduced to below 5%. The remaining solvent in the flour was separated by a vacuum oven (Memmert, Germany) at 40 °C for 24 h. The resulting flour was suspended in distilled water at a ratio of 1–10 (w/v), and the pH of the solution was adjusted to 11 by 1 N NaOH in order to open the protein structure, and then it was stirred for 1 h at room temperature by a magnetic stirrer (Jenway, UK). After that, centrifugation (Combi-514R, South Korea) was performed for 20 min at a speed of 5000 rpm and a temperature of 4 °C. The supernatants were collected, and the pH was set to 4 using 1 N hydrochloric acid. The centrifugation process was repeated at 5000 rpm for 20 min at a temperature of 4 °C. Finally, the resulting pellet was dried by a freeze dryer (FDB 5503, South Korea) and stored in closed containers in a dry and cool environment [4].

2.2.2. Microwave pretreatment

The protein solution of pumpkin seed protein concentrate (5% w/v) was prepared in 0.1 M phosphate buffer (100 g/l) (Na$_2$H-PO$_4$–NaH$_2$PO$_4$, pH 7.4). The solution was stirred for 30 min and exposed to microwave energy (Daewoo, South Korea) with a power of 450–900 W for 30–90 s. It should be noted that after measuring the total antioxidant activity, treatment at 600 W for 30 s was selected and applied as the optimal pretreatment. Protein solutions pre-treated with microwaves were used as substrate solutions in enzymatic hydrolysis experiments [17].

2.2.3. Enzymatic hydrolysis

In order to optimize the enzymatic hydrolysis conditions, the response surface methodology was used. Alcalase and pancreatin enzymes were added in ratios of 0.5–2.5% (v/w) of the protein substrate, and the hydrolysis time was determined as an independent factor for each within 20–190 min in a shaker incubator (VS-8480, South Korea) at a speed of 200 rpm. The temperature and pH of hydrolysis were considered according to the optimum temperature and pH of each enzyme (pancreatin: 40 °C and pH = 7.4; alcalase: 50 °C and pH = 8). In order to inactivate the enzyme, the protein solution was placed in a hot water bath (WNB 22, Germany) at a temperature of 85 °C for 15 min. Then, the supernatant was centrifuged (Combi-514R, South Korea) at 4000 rpm at 4 °C for 15 min. The resulting supernatant was freeze-dried to obtain PSPH powder and stored at −20 °C until use [18].

2.2.4. DPPH free radical scavenging activity

The hydrolysates were dissolved in distilled water at the optimal concentration (40 mg/ml). Then, 200 μl of the sample were mixed with 600 μl of methanol and 200 μl of DPPH (0.15 mM in methanol). After shaking vigorously for 2 min, it was kept at room temperature in a dark place for 30 min. The absorption was measured at 517 nm using a UV–vis (T80, UK) spectrophotometer. The control sample contained 800 μl of methanol and 200 μl of DPPH (0.15 mM). DPPH free radical scavenging activity was calculated according to Eq. (1) [19].

$$\text{DPPH } (\%) = (\text{Blank absorbance } - \text{ Sample absorbance})/\text{Blank absorbance} \times 100 \tag{1}$$

2.2.5. Fe chelation activity

200 μl of the sample was mixed with 10 μl of FeCl$_2$ (2 mM) and 600 μl of distilled water. Then 20 μl of ferrozine solution (5 mM) was added to the mixture and mixed vigorously for 2 min. After keeping the mixture at room temperature for 10 min, the color reduction due to iron chelation was recorded by measuring the absorbance at 562 nm. The control sample contained 800 μl of distilled water, 10 μl of FeCl$_2$, and 20 μl of ferrozine solution (5 mM). The chelation activity was calculated using Eq. (2) [19].

$$\text{Chelation activity } (\%) = (\text{Blank absorbance } - \text{ Sample absorbance})/\text{Blank absorbance} \times 100 \tag{2}$$

2.2.6. Total antioxidant activity

100 μl of the sample with 1 ml of reagent (0.6 M sulfuric acid, 28 mM sodium phosphate, and 4 mM ammonium molybdate) was added into an Eppendorf tube and placed in a 90 °C water bath for 90 min. After cooling the samples, their absorbance was recorded at 695 nm. The control sample was double-distilled water. The higher absorption rate indicated a higher total antioxidant activity [20].

2.3. Preparation of alginate-based delivery system

Hydrogel beads were prepared by the ion gelation method. First, a solution with a concentration of 2% of sodium alginate alone and with a combination of CMC-alginate was made in distilled water at a ratio of 20:80, and for complete hydration, it was mixed for 24 h. Then, 40 mg/ml of PSPH was added to the wall materials at a ratio of 1:1. To form beads, the resulting solution was added drop by drop to 20 ml of 5% calcium chloride solution using a 2 ml syringe. The beads were kept in the solution for an hour. Then, the beads were separated from the solution and washed with distilled water. Some beads were lyophilized (FDB 5503, South Korea), and the rest were analyzed immediately [21].

2.4. Preparation of chitosan-coated alginate-based delivery system

Coating with chitosan was done according to the ionotropic/external gelation method. A specific weight of beads was added to 20 ml of 0.1%, 0.2%, and 0.3% chitosan solutions, which dissolved in 1% acetic acid. They were stirred by a magnetic stirrer (Jenway, England) for 15 min at a speed of 50 rpm. Then, it was separated by a steel mesh, and part of the beads were lyophilized (FDB 5503, South Korea), and the rest were immediately analyzed [22].

2.5. Encapsulation efficiency

100 mg of beads were mixed with 1 ml of 0.1 M potassium phosphate buffer (pH = 8) and stirred for 15 min using a vortex. The beads were separated from the dispersion by a centrifuge (Combi-514R, South Korea) at a speed of 15,000 rpm for 20 min. The supernatant was diluted properly and analyzed by the Bradford method at a wavelength of 595 nm. Encapsulation efficiency was measured by Eq. (3) [23].

$$\text{Encapsulation efficiency } (\%) = C_T - C_S/C_T \times 100 \tag{3}$$

where C_T was the total protein content and C_S was the supernatant protein content.

2.6. Fourier transform infrared (FT-IR)

The IR analysis of hydrolysates and loaded beads was done by a FTIR spectrophotometer. The samples were crushed with potassium bromide, and spectral scanning was done in the range of 400–4000 cm^{-1} [24].
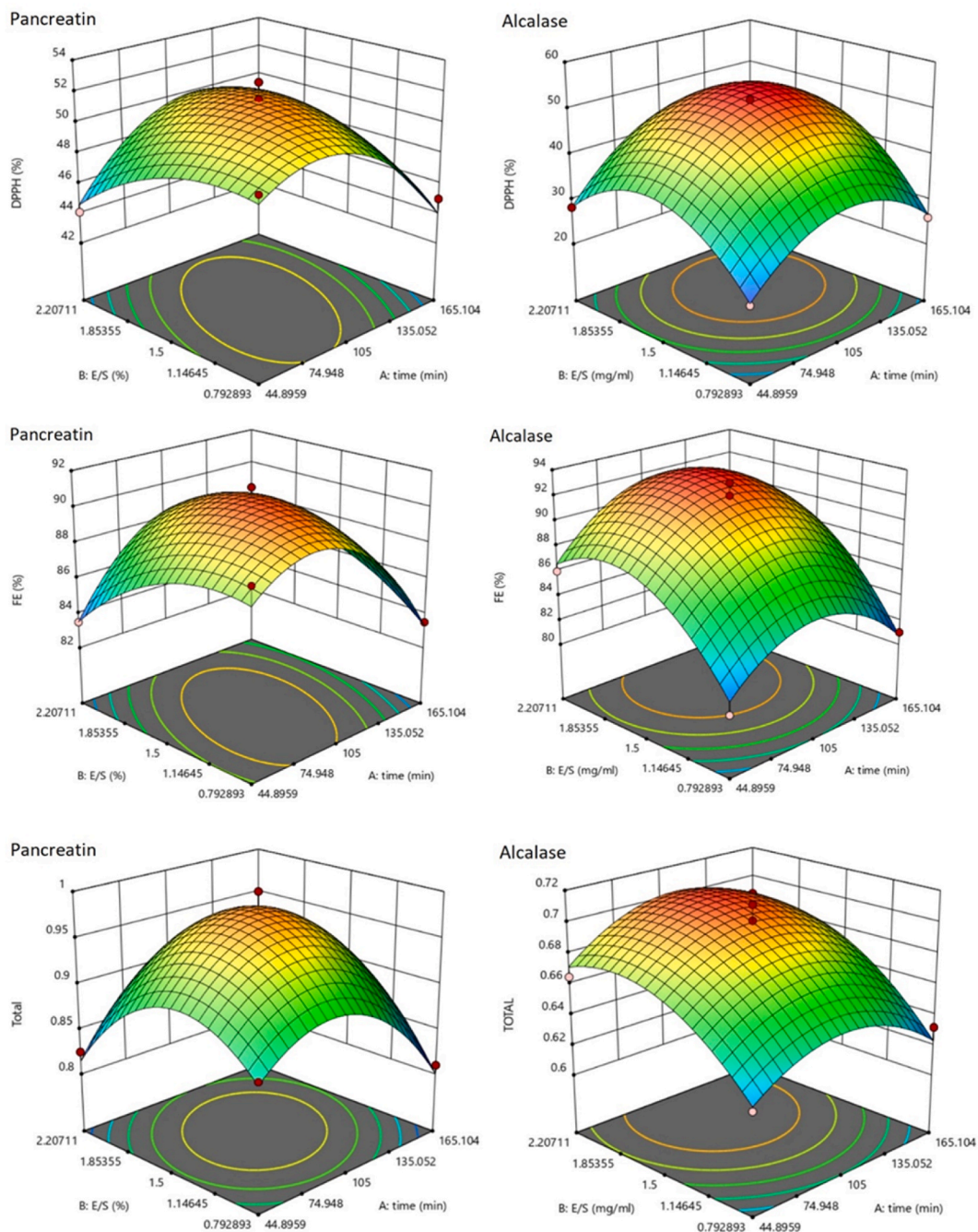

Fig. 1. Effect of hydrolysis conditions on the antioxidant activity of pumpkin seed protein hydrolysates.

2.7. Zeta potential, particle size and PDI

Zeta potential, average particle size and particle dispersion index (PDI) were measured after diluting samples with distilled water using a zeta sizer and the dynamic light scattering technique [25,26].

2.8. Scanning electron microscope (SEM)

The morphological structure of the samples was determined by scanning electron microscopy (SEM) at a voltage of 10 kv. Freeze-dried samples were coated with gold (Au) and then analyzed [21].

2.9. Swelling

1 g of beads was immersed in 20 ml of the simulated gastrointestinal medium (Simulated gastric fluid (SGF) contained 0.2 g of sodium chloride and 0.32% pepsin, with a final pH of 2, and simulated intestinal fluid (SIF) contained 0.1% pancreatin and 50 mM potassium dihydrogen phosphate, with a final pH of 7.4) and placed in a shaker incubator (VS-8480, South Korea) at a speed of 100 rpm and a temperature of 37 °C. After the digestion time (in a gastrointestinal environment), the beads were separated from the medium, gently wiped with filter paper, and weighed. The change in the weight of beads was determined using Eq. (4) [27].

$$\text{Swelling } (\%) = W_S - W_B/W_S \times 100 \tag{4}$$

where W_S was the weight of swollen beads and W_B was the weight of dry beads.

2.10. Release rate in simulated gastrointestinal digestion

Simulated gastric fluid (SGF) contained 0.2 g of sodium chloride and 0.32% pepsin, with a final pH of 2, and simulated intestinal fluid (SIF) contained 0.1% pancreatin and 50 mM potassium dihydrogen phosphate, with a final pH of 7.4 [28]. The release rate was calculated using the method of Azad, Al-Mahmood [29]. Briefly, 1 g of beads was added to 10 ml of simulated gastric medium. Then, incubation was done at 37 °C at a speed of 50 rpm for 2 h. Sampling was done every 30 min. Finally, the release rate was determined using the Bradford method. After that, 10 ml of simulated intestinal solution was added to 1 g of each sample, which was also continuously shaken at a speed of 50 rpm 37 °C and incubated for 4 h. Sampling was done every 60 min. Finally, the release rate was evaluated using the Bradford method.

2.11. Statistical analysis

Enzymatic hydrolysis was done using Design Expert software version 11 and response surface methodology in the form of central compound design. Data analysis was done with SPSS software version 26, in the form of a completely randomized design using one-way analysis of variance (ANOVA). The comparison of averages was checked with Duncan's multi-range test at a 95% confidence level, and graphs were drawn with Excel 2019 and Origin 2019 software. All tests were performed in three replications.

3. Results and discussion

3.1. Antioxidant activity of PSPH

According to Fig. 1, the highest amount of antioxidant activity for pancreatin and alcalase hydrolysate based on DPPH free radical scavenging activity, iron chelation activity, and total antioxidant activity (absorbance at 695 nm) was 52.6%, 91.1% and 1.0, and 52%, 93% and 0.711, respectively. The highest amount of antioxidant activity belonged to the time of 105 min and the ratio of 1.5% E/S. In other words, antioxidant activity decreased with time. Nevertheless, the continuous process of hydrolysis, together with the effects of enzymes on early-stage hydrolysates, may have led to the destruction of high-capacity antioxidants [30]. According to Kaveh, Sadeghi [31], as time went on, there was a decrease in antioxidant activity. On the other hand, increasing enzyme concentration to 1.5% resulted into a decrease in antioxidant activity. This results from excessive protein hydrolysis, leading to the complete release of hydrophilic amino acids that cannot react with fat-soluble DPPH free radicals [32]. Moreover, higher levels of E/S might destroy the electron-donating characteristics and Fe chelation activities, which reduce their antioxidative properties. Based on the results, pancreatin's hydrolysates had more anti-oxidant activities in DPPH free radical scavenging and total anti-oxidant activities; therefore, this sample was selected for encapsulation purposes.

3.2. Encapsulation efficiency

The highest amount of encapsulation efficiency belonged to the CMC-alginate-chitosan sample (91.4 ± 3.6%) and the lowest amount belonged to the alginate sample (71.63 ± 2.15%). Also, it was 85.06 ± 2.54%, 81.4 ± 2.8% in CMC-alginate and alginate-chitosan beads, respectively. Generally, the microcapsulation efficiency of all samples was more than 70%, which shows the appropriate ability of the hydrogel network produced to load protein hydrolysate. The reason for this could be that an egg box made from

Ca^{2+} ions and sodium alginate with proper densities forms a dense structure that contains appropriate channels for protein hydrolysate ingress and loading into the hydrogel medium [33]. Calcium alginate hydrogel has inherent brittleness and poor mechanical properties. CMC has many hydroxyl groups, which, apart from high water absorption, can form hydrogen bonds with alginate molecules to enhance the stability of the hydrogel material. It is evident that the samples coated with chitosan have higher encapsulation efficiency than those without, which corresponds to the fact that cationic chitosan chains interact strongly with anionic sodium alginate and CMC groups, thereby efficiently covering the surface of alginate beads, resulting in a more uniform gel network with better ability for bioactive compounds loadings [34]. Similar to these results, Krasaekoopt and Watcharapoka [35] reported that using chitosan coating on alginate beads loaded with Lactobacillus acidophilus significantly increased the microcapsulation efficiency. Also, Bhopatkar, Anal and Stevens [36] reported the positive effect of chitosan coating on the micro-coating efficiency of alginate beads containing hemoglobin.

3.3. Fourier transform infrared (FTIR)

According to Fig. 2A, the spectra showed stretching vibrations of O–H bonds and asymmetric and symmetric stretching vibrations of the carboxylate group in 3400, 1600, and 1400 (cm^{-1}), respectively. In addition, the spectra showed C–O stretching vibrations in the range of 1000–1100 (cm^{-1}). The 2100 (cm^{-1}) vibration was attributed to the symmetric O–H stretching. The spectra of protein hydrolysates showed that the vibrations of 3400 (cm^{-1}) belonged to NH and O–H stretching, the 2200 (cm^{-1}) belonged to C=C groups, and the 1600, 1400, and 1000 (cm^{-1}) vibrations belonged to C=O stretching and NH bending groups in the first type amide, COO$^-$ stretching in the third type amide, and C–O stretching, respectively. The stretching observed at the lower wavelength belonged to the carbohydrate fraction, which represented the COH group. According to chitosan spectroscopy, the vibrations of 3400 (cm^{-1}) were related to N–H and O–H stretching. The peak of, 2800 (cm^{-1}) can be attributed to asymmetric C–H stretching. The remaining N-acetyl groups were seen by the bands at 1600 (cm^{-1}) C=O stretching of amide I and 1300 (cm^{-1}) C–N stretching of amide III, respectively. The peak of 1000–1100 (cm^{-1}) was related to C–O stretching. The results were similar to the previous reports of Daemi and Barikani [37], Araujo, Cortese [38], Lu, Peng [39], and Queiroz, Teodosio Melo [40]. According to Fig. 2B, After bead formation, FTIR analysis showed the appearance of 2127.97–2126.63 cm^{-1} peaks in uncoated alginate and CMC-alginate, respectively, which probably indicate hydrogen and electrostatic interactions between carboxyl groups of polysaccharides with protein hydrolysate and CaCl$_2$. The diffusion of calcium ions in the alginate network was confirmed by the change of vibrations in alginate and CMC-alginate beads, 1641.95 and 1640.24 cm^{-1} to 1635.03 and 1635.54 cm^{-1} (to lower levels), respectively [41]. The penetration of CMC in alginate caused the characteristic peak of OH stretching vibration to decrease from 3424.15 to 3410.58 cm^{-1}. In addition, the formation of new intermolecular hydrogen bonds between the two polymers increased the peak width [42]. In chitosan-coated beads, when chitosan was added to the sodium alginate bead, the peak of 1654.59 cm^{-1} corresponding to chitosan amid-I was shifted to a lower level of 1626.68 cm^{-1} in the chitosan-alginate bead. On the other hand, the electrostatic interaction between the protonated amine groups of chitosan and the carboxylate groups of CMC affected the stretching vibration of NH$_2$ in chitosan. The peak of 1654.59 cm^{-1} in chitosan was shifted to a lower level of 1626.24 cm^{-1} in CMC-alginate-chitosan [43]. The 3436.89 cm^{-1} peak in chitosan increased to 3751.75 cm^{-1}, due to the formation of new hydrogen bonds between the hydroxyl group of CMC and the skeletal oxygen groups of sodium alginate and chitosan [41]. It should be noted that the beads contained peaks in the range of 1151.52–1114.29 cm^{-1}, which indicated the presence of hydrophilic compounds in protein hydrolysate [44]. Also, the peaks in the range of 564.86–574.49 cm^{-1} indicated the
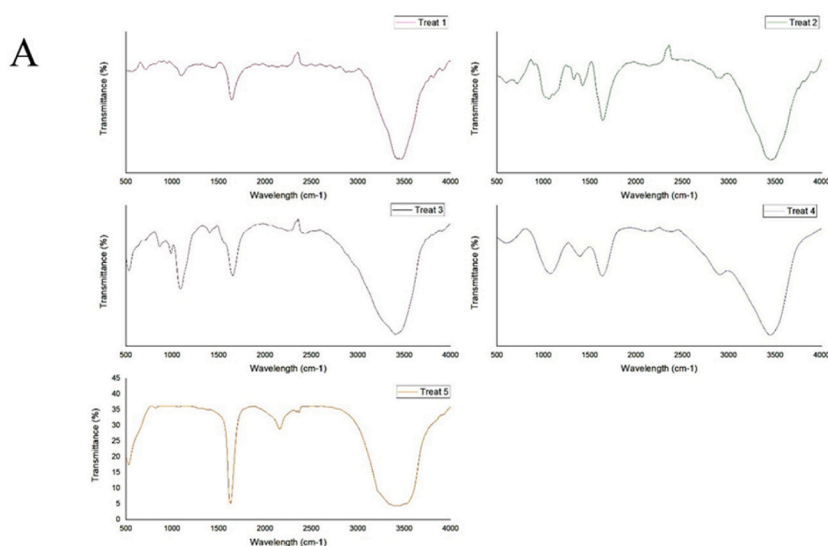

Fig. 2A. FTIR spectra of free components. Treat 1: Sodium alginate; Treat 2: CMC; Treat 3: Pumpkin seed protein hydrolysate; Treat 4: Chitosan; and Treat 5: CaCl2.
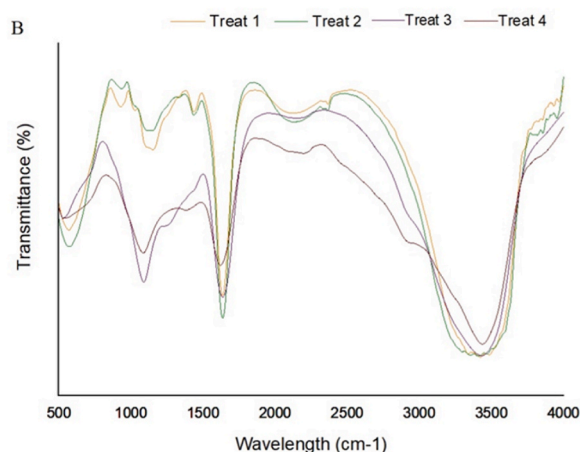
Fig. 2B. FTIR spectra of Treat 1: Alginate loaded with PSPH; Treat 2: CMC-alginate loaded with PSPH; Treat 3: chitosan-alginate loaded with PSPH and Treat 4: chitosan-CMC-alginate loaded with PSPH.

formation of S–O and S–S bonds [45]. In general, the establishment of hydrogen bonds and electrostatic interactions indicates the successful loading of hydrolysate proteins into hydrogels.

3.4. Zeta potential, particle size and PDI

The quantitative measurement of the charge of colloidal particles in liquid suspension is called the zeta potential [46]. Similar to previous reports by Zhang, Zhang [47], and Silverio, Sakanaka [26], the zeta potential of the sodium alginate solution (-57.21 ± 0.63) was negative. This negative value is attributed to the separated carboxyl groups of guluronic and mannuronic acids that exist in the alginate molecule. The negative charge of the CMC and sodium alginate solution (-73.39 ± 0.85) is due to the separation of Na^+ ions from carboxylic groups [48]. The zeta potential of protein hydrolysate (-4.36 ± 0.35) was similar to the findings of Lu, Peng [39]. Protein hydrolysate can interact with biopolymer molecules through electrostatic interactions to make hydrogels and affect their maintenance and release properties [47]. The zeta potential of chitosan ($+33.40 \pm 0.8$) was due to the presence of NH^{3+} groups, which was similar to the findings of Yousefi, Khanniri [49]. Generally, zeta potential values greater than 30 mv and less than -30 mv are usually used to prevent particle aggregation or coagulation in aqueous solutions [50]. Nevertheless, the zeta potential obtained considering the particle size of the microcapsules was considered sufficient because, in micrometer-size, the effect of zeta potential on colloidal stability is not as critical as in nanometer-size [51]. According to Table 1, The charge of the uncoated microparticles showed a significant decrease compared to polysaccharide solutions, which indicated the ionic association between the carboxyl groups and the calcium ions, which was also reported by Maestrelli, Cirri [52]. Zeta potential increased in chitosan-coated beads (ionotropic method) compared to uncoated beads. Also, the results were similar to the findings of Li, Kong [53]. Probably, the interactions between the cationic groups of chitosan and $CaCl_2$ and the anionic groups of alginate and CMC led to this charge increase.

The size of the particles in a carrier system plays an important role in the bioavailability of the encapsulated compound [54]. It should be noted that the smaller the particle, the higher the stability of the emulsion. According to Table 1, The particle size in CMC-alginate beads was greater than alginate beads, which can probably be attributed to the distinct molecular structures of the two polysaccharides, the addition of CMC to the alginate formulation, and their intermolecular interactions [55]. The average size of chitosan-coated particles was larger than that of uncoated particles, which was similar to the previous findings of Li, Kong [53], and Khorshidian, Mahboubi [25].

The distribution and uniformity of particle size are shown by the dispersion index (PDI), and its value varies from 0 to 1 depending on the type of system [56]. This index in higher values indicates a wide size distribution of particles and rough and non-uniform masses in the system, and its lower values indicate the uniformity and homogeneity of the particle size [57]. According to Table 1, the dispersion index of the samples was in the range of 0.45–0.49, which indicates the homogeneity of the samples and a uniform distribution of particle size. The results are similar to the reports of Khorshidian, Mahboubi [25].

Table 1
Zeta potential, particle size and PDI of microparticles.

Indicators	Treat 1	Treat 2	Treat 3	Treat 4
Zeta potential (mv)	-9.17 ± 0.21^c	-12.1 ± 0.34^d	11.8 ± 0.25^a	8.2 ± 0.18^b
Particle size (μm)	75 ± 0.18^d	90 ± 0.23^c	125 ± 0.29^b	153 ± 0.35^a
PDI	0.45 ± 0.01^a	0.47 ± 0.01^a	0.48 ± 0.03^a	0.49 ± 0.05^a

Treat 1: alginate beads; Treat 2: CMC-alginate beads; Treat 3: alginate-chitosan beads; and Treat 4: CMC-alginate-chitosan beads. All beads are loaded by PSPH. Similar letters mean there is no significant difference (p > 0.05).

3.5. Scanning electron microscopy (SEM)

Fig. 3 shows the scanning electron microscopy images of alginate beads that are uncoated and coated with chitosan. Figures of plain alginate (A, a) and CMC-alginate (C, c) showed that beads without chitosan coating have smooth surfaces, while those that contain chitosan coating show wrinkled surfaces. Meanwhile, all the beads were practically spherical. Surface morphology analysis between uncoated beads showed that CMC-alginate has a smoother, more polished and non-porous surface than plain alginate. It should be noted that in the samples with chitosan coating, the CMC-alginate-chitosan (D, d) sample showed less shrinkage than the alginate-chitosan (B, b) sample. The shrinkage of alginate beads coated with chitosan has been confirmed by previous studies [58]. With the increase in alginate concentration, the porosity of the beads increased. The porosity changed according to the composition of the hydrogel, which led to differences in the shape and surface of the beads [59]. The greater negative charge of CMC-alginate and more interactions with the positive charge of chitosan could be the reason for the less shrinkage of CMC-alginate.

3.6. Swelling rate in the simulated gastrointestinal digestion

According to Fig. 4A, the highest amount of swelling in the gastric environment belonged to the concentration of 0.1% chitosan in the CMC-alginate-chitosan sample ($-19.6 \pm 0.16\%$), and the lowest amount belonged to the concentration of 0.3% chitosan in the alginate-chitosan sample ($-36.32 \pm 0.11\%$). According to Fig. 4B, the highest amount of swelling in the intestinal environment belonged to the concentration of 0.1% chitosan in the CMC-alginate-chitosan sample ($35.2 \pm 0.3\%$), and the lowest amount belonged to the concentration of 0.3% chitosan in the alginate-chitosan sample ($15.4 \pm 0.21\%$). In both environments, the swelling amount of alginate-chitosan was lower than the CMC-alginate-chitosan samples, and with the increase in chitosan concentration, the swelling amount decreased. The swelling rate of beads with higher cross-links is lower than that of those with fewer cross-links. In an acidic environment, due to the formation of strong hydrogen bonds between alginate (-COOH and –OH) and chitosan (-NH2) groups, as well
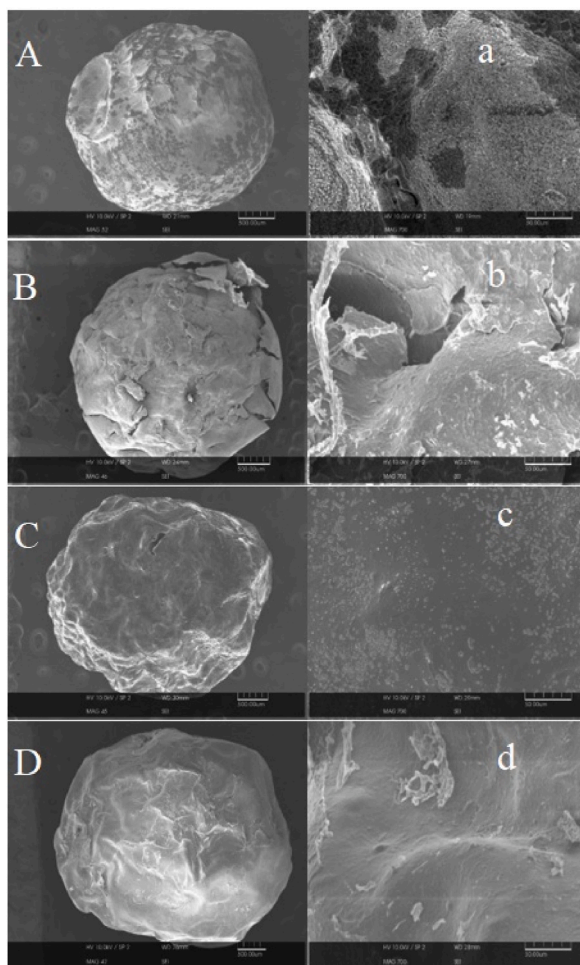

Fig. 3. SEM images of A, a: alginate; B, b: chitosan-alginate; C, c: CMC-alginate; and D, d: chitosan-alginate-CMC (all beads are loaded with protein hydrolysate). Capital letters indicate 50 magnification, and small letters indicate 700 magnification.
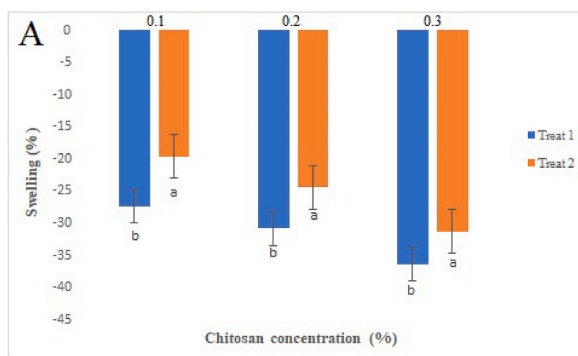
Fig. 4A. Swelling amount of samples in a simulated gastric condition. Treat 1: Alginate-chitosan, and Treat 2: CMC-alginate-chitosan. Data represent the mean value ± SD of at least n = 3. Similar letters mean there is no significant difference (p > 0.05).
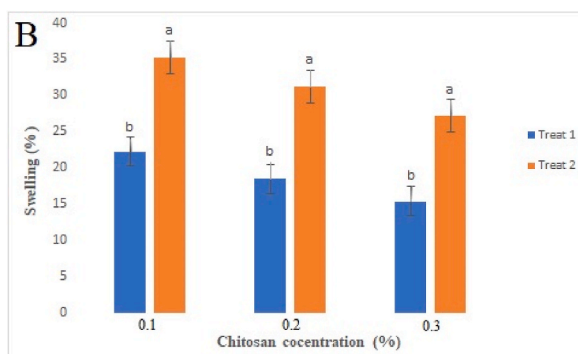

Fig. 4B. Swelling amount of samples in a simulated intestinal condition. Treat 1: Alginate-chitosan, and Treat 2: CMC-alginate-chitosan. Data represent the mean value ± SD of at least n = 3. Similar letters mean there is no significant difference (p > 0.05).

as the protonation of the carboxyl groups, the swelling rate and the network potential to absorb solvents from the surrounding environment decreased [60]. In addition, in this environment, calcium ions are separated and form calcium phosphate salts, which no longer cross-link with the alginate matrix and lead to the destruction of the hydrogel network [61]. The instability of the alginate polymer network at intestinal pH is due to the ionic repulsion between Na^+ and Ca^{2+} ions within hydrogel beads [62]. Conversely, ionization of alginate at intestinal pH generates electrostatic repulsive forces among alginate chains, thereby enhancing swelling [63]. The addition of chitosan to alginate leads to the formation of a more complex system, which is created by the mixing of both polymers and the formation of polyelectrolyte complexes between the amino groups of chitosan and carboxylate groups of alginate [64]. These features enhance the stability of alginate-chitosan hydrogel and increase resistance to osmotic pressure [61].
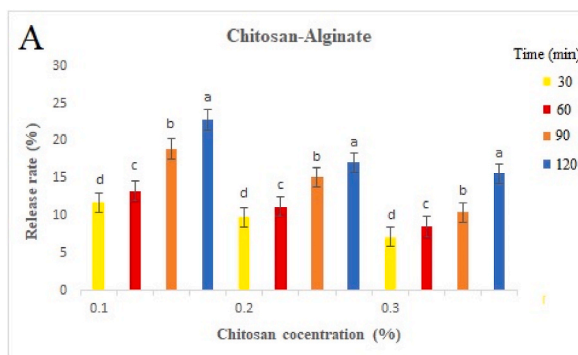

Fig. 5A. Release pattern of Chitosan-Alginate in simulated gastric digestion. Data represent the mean value ± SD of at least n = 3. Similar letters mean there is no significant difference (p > 0.05).

3.7. Release rate in the simulated gastrointestinal digestion

According to Fig. 5A and Fig. 5B, the release amount of alginate-chitosan and CMC-alginate-chitosan hydrogel in gastric conditions increased over time and reached its maximum amount in 120 min ($22.8 \pm 0.4\%$ and $15.53 \pm 0.14\%$, respectively, in chitosan-alginate and chitosan-alginate-CMC). On the other hand, with the increase in chitosan concentration, the release rate in gastric conditions decreased, and at a concentration of 0.3%, the lowest release rate ($7.13 \pm 0.1\%$ and $3.5 \pm 0.05\%$, respectively, in chitosan-alginate and chitosan-alginate-CMC) was obtained. At a concentration of 0.3% chitosan, there was no significant difference in the release rate of chitosan-alginate-CMC hydrogel in 90 and 120 min ($p > 0.05$). It should be noted that the alginate-chitosan sample showed a higher release amount in the gastric environment than CMC-alginate-chitosan. According to Fig. 6A and Fig. 6B, in both samples, the amount of release in the intestinal environment increased with the passage of time, and the highest amount belonged to 240 min ($50.9 \pm 0.84\%$ and $38.1 \pm 0.53\%$, respectively, in chitosan-alginate and chitosan-alginate-CMC). On the other hand, with the increase in chitosan concentration, the release rate decreased, and the lowest release rate ($15.03 \pm 0.13\%$ and $9.76 \pm 0.11\%$, respectively, in chitosan-alginate and chitosan-alginate-CMC) was obtained at a concentration of 0.3% chitosan. At the concentration of 0.2% chitosan, there was no significant difference in the release of chitosan-alginate-CMC hydrogel between 180 and 240 min ($p > 0.05$). The release amount in the chitosan-alginate sample was higher than that in the chitosan-alginate-CMC. Physical hydrogels, such as calcium alginate, have disadvantages such as instability and rapid dissolution [65]. The use of hydrogels made with a single network and microporous structure is limited due to the problem of leakage because they cannot effectively maintain the bioactive compound at stable and desirable levels for a long period of time [66]. Therefore, in order to solve the problem caused by the structure of microporous hydrogels, smart multi-component hybrid hydrogel structures have become a potentially effective strategy [67]. The amine groups of chitosan are able to be protonated with the carboxyl group of alginate and form a gel through electrostatic interaction [68]. Chitosan establishes strong electrostatic interactions and hydrogen bonding with carboxymethyl cellulose to form a gel [69]. Probably, the amount of electrostatic interactions in alginate-chitosan and CMC-alginate-chitosan hydrogels caused the differences in structure stability and release rates in the two samples. The protective effect of chitosan and the covering of the pores in the alginate hydrogel network prevent the rapid release of loaded compounds in acidic conditions [70]. Under acidic pH, the carboxyl groups of alginate are protonated and become COOH, which is the cause of the formation of alginic acid and the strength of the alginate matrix [71]. Alginate hydrogels shrink at an acidic pH, and the electrostatic interaction between alginate and chitosan allows the protonation of amine groups [72] and prevents the release of the loaded compound from the beads. Also, more release in the intestinal environment is due to the swelling of alginate, deprotonation, negative charge of chitosan, and increased repulsion of negative charges [72]. Moreover, the high affinity of phosphate ions, which are present in the intestinal fluid for Ca^{+2}, disrupts the calcium-alginate gel matrix [25].

3.8. Antioxidant activity after simulated gastrointestinal condition

The amount of antioxidant activity after release in the simulated gastric and intestinal conditions was evaluated by two methods: DPPH free radical scavenging activity and iron chelation activity. According to Fig. 7A and Fig. 7B, in the simulated gastric environment, the highest amount of DPPH free radical scavenging and iron chelation activity belonged to the concentration of 0.3% chitosan ($12.1 \pm 0.17\%$ and $18.56 \pm 0.3\%$, respectively) of chitosan-alginate hydrogel, and the lowest amount belonged to chitosan-alginate-CMC with a concentration of 0.1% chitosan ($3.8 \pm 0.05\%$ and $7.03 \pm 0.1\%$, respectively). On the other hand, according to Fig. 8A and B, in the simulated intestinal environment, the highest amount of DPPH free radical scavenging and iron chelation activity belonged to the concentration of 0.3% chitosan ($91.63 \pm 0.9\%$ and $94.83 \pm 0.93\%$, respectively) in chitosan-alginate hydrogel, and the lowest amount belonged to chitosan-alginate-CMC with a concentration of 0.1% chitosan ($61.53 \pm 0.7\%$ and $76.2 \pm 0.83\%$, respectively). According to Fig. 8B, the amount of iron chelation activity in the chitosan-alginate-CMC sample with a concentration of 0.3% of chitosan was not significantly different from the chitosan-alginate sample with a concentration of 0.2% of chitosan ($p > 0.05$). Most importantly, the highest amount of antioxidant activity belonged to chitosan-alginate in both simulated environments, and the level of antioxidant activity increased with increasing the chitosan concentration. The possible reason for the higher level of antioxidant activity in alginate-chitosan hydrogel compared to CMC-alginate-chitosan is due to the strong interactions between polymers [73], which affect the stability of the structure, release rate, and level of antioxidant activity. Moreover, chitosan, as a protective layer, prevents the impact of adverse environmental factors such as temperature and light on the loaded composition [74]. On the other hand, the higher antioxidant activity with increasing chitosan concentration is probably due to the antioxidant ability of chitosan by itself, which is similar to the findings of Reyhani Poul and Yeganeh [75] and Sankar, Ramesh [76]. The result indicated that chitosan coating on alginate-based microgels can improve the stability of microparticles, protect PSPH from destruction, and delay the release rate of PSPH from these microparticles.

4. Conclusion

According to the results, PSPH has antioxidant activity that can be used in food formulation and food supplement production. Since micro-coating is an effective method of preserving bioactive compounds against degradation and adverse environmental conditions, this method was used. Due to the leakage of compounds from the alginate hydrogel and because of its fragile structure, it was coated with chitosan. The results showed that, in the SGI environment, the swelling amount of alginate-chitosan was lower than the CMC-alginate-chitosan sample, and with the increase in chitosan concentration, the swelling amount decreased. The release amount in the alginate-chitosan sample was higher than that in CMC-alginate-chitosan. It should be noted that, with the increase in chitosan
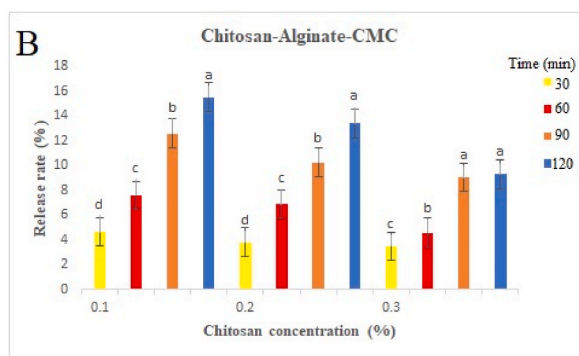
Fig. 5B. Release pattern of Chitosan-Alginate-CMC in simulated gastric digestion. Data represent the mean value ± SD of at least n = 3. Similar letters mean there is no significant difference (p > 0.05).
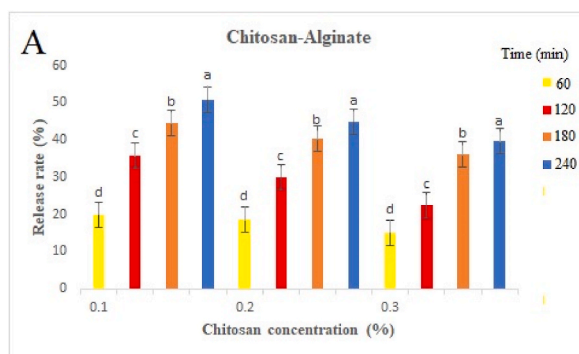

Fig. 6A. Release pattern of Chitosan-Alginate in simulated intestinal digestion. Data represent the mean value ± SD of at least n = 3. Similar letters mean there is no significant difference (p > 0.05).
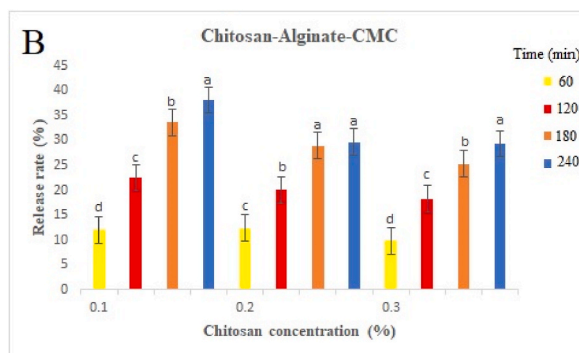

Fig. 6B. Release pattern of Chitosan-Alginate-CMC in simulated intestinal digestion. Data represent the mean value ± SD of at least n = 3. Similar letters mean there is no significant difference (p > 0.05).

concentration, the release rate decreased. Also, the amount of release increased with the passage of time. The highest amount of antioxidant activity belonged to the alginate-chitosan sample in both simulated environments, and the level of antioxidant activity increased with increasing the chitosan concentration, which is probably due to the antioxidant ability of chitosan by itself. FTIR spectroscopy of alginate and alginate-CMC hydrogels before and after chitosan coating showed the same absorption peaks and did not differ from each other, which shows the successful loading of hydrolysate protein into hydrogels. Findings showed that chitosan coating can improve the stability of alginate-based microgels and improve the release behavior of bioactive compounds from them.
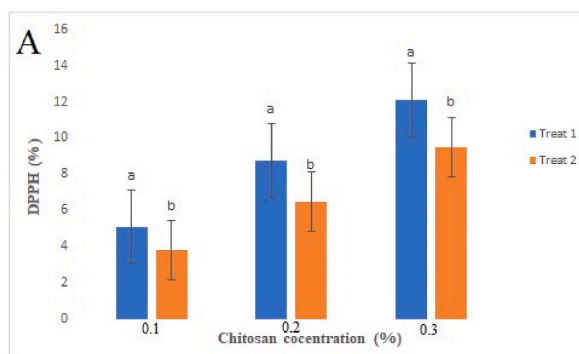
Fig. 7A. DPPH free radical scavenging activity of Treat 1: chitosan-alginate and Treat 2: chitosan-alginate-CMC after release in simulated gastric digestion. Data represent the mean value $\pm$ SD of at least n = 3. Similar letters mean there is no significant difference (p > 0.05).
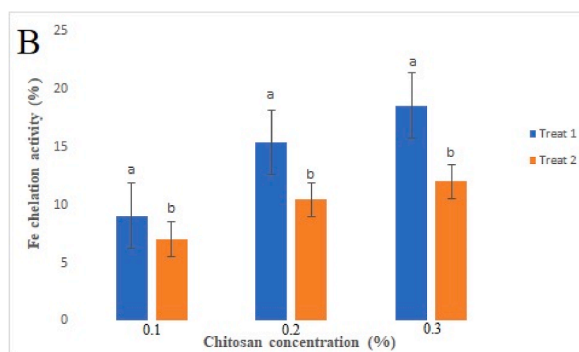

Fig. 7B. Fe chelation activity of Treat 1: chitosan-alginate and Treat 2: chitosan-alginate-CMC after release in simulated gastric digestion. Data represent the mean value $\pm$ SD of at least n = 3. Similar letters mean there is no significant difference (p > 0.05).
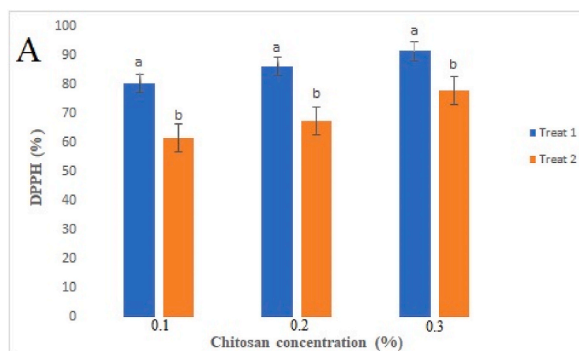

Fig. 8A. DPPH free radical scavenging activity of Treat 1: chitosan-alginate and Treat 2: chitosan-alginate-CMC after release in simulated intestinal digestion. Data represent the mean value $\pm$ SD of at least n = 3. Similar letters mean there is no significant difference (p > 0.05).

CRediT authorship contribution statement

Zeinab Nooshi Manjili: Writing – original draft, Software, Resources, Investigation, Funding acquisition, Formal analysis. **Alireza Sadeghi Mahoonak:** Writing – review & editing, Validation, Supervision, Conceptualization, Visualization. **Mohammad Ghorbani:** Writing – review & editing. **Hoda Shahiri Tabarestani:** Writing – review & editing.

Declaration of competing interest

The authors declare that they have no known competing financial interests or personal relationships that could have appeared to
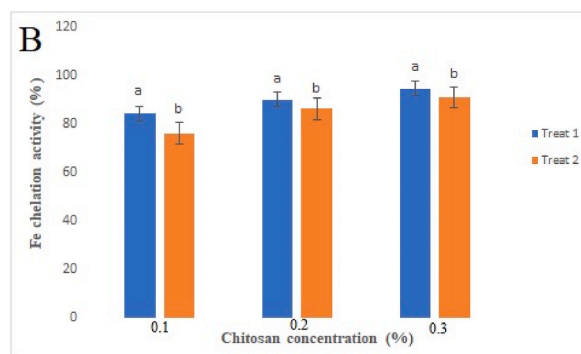
Fig. 8B. Fe chelation activity of Treat 1: chitosan-alginate and Treat 2: chitosan-alginate-CMC after release in simulated intestinal digestion. Data represent the mean value ± SD of at least n = 3. Similar letters mean there is no significant difference (p > 0.05).

influence the work reported in this paper.

Acknowledgements

References

[1] H. Korhonen, A. Pihlanto, Bioactive peptides: production and functionality, Int. Dairy J. 16 (9) (2006) 945–960.
[2] S. Fan, et al., Optimization of preparation of antioxidative peptides from pumpkin seeds using response surface method, PLoS One 9 (3) (2014) e92335.
[3] K. Zakeri, et al., Optimization of hydrolysis condition of pumpkin seeds with alcalase enzyme to Achieve maximum antioxidant and nitric oxide inhibition activity, Research and Innovation in Food Science and Technology 7 (4) (2019) 445–458.
[4] S.N. Mazloomi-Kiyapey, et al., Production of antioxidant peptides through hydrolysis of medicinal pumpkin seed protein using pepsin enzyme and the evaluation of their functional and nutritional properties, Arya Atherosclerosis 15 (5) (2019) 218.
[5] J.L. Guía-García, et al., Micro and nanoencapsulation of bioactive compounds for agri-food applications: a review, Ind. Crop. Prod. 186 (2022) 115198.
[6] Díaz-Torres, R.D.C., et al., Bioactive compounds obtained from plants, their pharmacological applications and encapsulation, in *Phytomedicine*. 2021, Elsevier. p. 181-205.
[7] P. Shah, Polymers in food, in: Polymer Science and Innovative Applications, Elsevier, 2020, pp. 567–592.
[8] H. Zheng, et al., pH-sensitive alginate/soy protein microspheres as drug transporter, J. Appl. Polym. Sci. 106 (2) (2007) 1034–1041.
[9] K.Y. Lee, D.J. Mooney, Alginate: properties and biomedical applications, Prog. Polym. Sci. 37 (1) (2012) 106–126.
[10] F. Hossain, et al., Antifungal activities of combined treatments of irradiation and essential oils (EOs) encapsulated chitosan nanocomposite films in in vitro and in situ conditions, Int. J. Food Microbiol. 295 (2019) 33–40.
[11] Y. Zhang, et al., Synthesis of multiresponsive and dynamic chitosan-based hydrogels for controlled release of bioactive molecules, Biomacromolecules 12 (8) (2011) 2894–2901.
[12] C. Chang, et al., Superabsorbent hydrogels based on cellulose for smart swelling and controllable delivery, Eur. Polym. J. 46 (1) (2010) 92–100.
[13] H. Kono, Characterization and properties of carboxymethyl cellulose hydrogels crosslinked by polyethylene glycol, Carbohydr. Polym. 106 (2014) 84–93.
[14] A.S. Hoffman, Hydrogels for biomedical applications, Adv. Drug Deliv. Rev. 64 (2012) 18–23.
[15] S. Masoomi Dezfooli, et al., Chitosan coated alginate beads as probiotic delivery system for New Zealand black footed abalone (Haliotis iris), J. Appl. Polym. Sci. 139 (29) (2022) e52626.
[16] E. Alaa, Chitosan-coated alginate microbeads improve the anti-inflammatory potential of Etodolac: optimization using Box-Behnken design, in-vitro drug release and in-vivo study, Journal of advanced Biomedical and Pharmaceutical Sciences (2023) 133–144.
[17] B.F.C.A. Gohi, et al., Microwave pretreatment and enzymolysis optimization of the Lotus seed protein, Bioengineering 6 (2) (2019) 28.
[18] E. Nourmohammadi, et al., The optimization of the production of anti-oxidative peptides from enzymatic hydrolysis of Pumpkin seed protein, Iranian Food Science and Technology Research Journal 13 (1) (2017) 14–26.
[19] K.D. Kanbargi, S.K. Sonawane, S.S. Arya, Encapsulation characteristics of protein hydrolysate extracted from Ziziphus jujube seed, Int. J. Food Prop. 20 (12) (2017) 3215–3224.
[20] P. Prieto, M. Pineda, M. Aguilar, Spectrophotometric quantitation of antioxidant capacity through the formation of a phosphomolybdenum complex: specific application to the determination of vitamin E, Anal. Biochem. 269 (2) (1999) 337–341.
[21] Q. Li, et al., Fabrication and characterization of Ca (II)-alginate-based beads combined with different polysaccharides as vehicles for delivery, release and storage of tea polyphenols, Food Hydrocolloids 112 (2021) 106274.
[22] L. Segale, et al., Calcium alginate and calcium alginate-chitosan beads containing celecoxib solubilized in a self-emulsifying phase, Sci. Tech. Rep. 2016 (2016).
[23] A. Maqsoudlou, et al., Stability and structural properties of bee pollen protein hydrolysate microencapsulated using maltodextrin and whey protein concentrate, Heliyon 6 (5) (2020) e03731.
[24] R. Stoica, S. Pop, R. Ion, Evaluation of natural polyphenols entrapped in calcium alginate beads prepared by the ionotropic gelation method, J. Optoelectron. Adv. Mater. 15 (7–8) (2013) 893–898.
[25] N. Khorshidian, et al., Chitosan-coated alginate microcapsules loaded with herbal galactagogue extract: formulation optimization and characterization, Iran. J. Pharm. Res. (IJPR): IJPR 18 (3) (2019) 1180.
[26] G.B. Silverio, et al., Production and characterization of alginate microparticles obtained by ionic gelation and electrostatic adsorption of concentrated soy protein, Ciência Rural. 48 (2018).
[27] S.K. Wong, et al., In vitro digestion and swelling kinetics of thymoquinone-loaded pickering emulsions incorporated in alginate-chitosan hydrogel beads, Front. Nutr. 8 (2021) 752207.
[28] L. Basiri, G. Rajabzadeh, A. Bostan, α-Tocopherol-loaded niosome prepared by heating method and its release behavior, Food Chem. 221 (2017) 620–628.
[29] A.K. Azad, et al., Encapsulation of black seed oil in alginate beads as a ph-sensitive carrier for intestine-targeted drug delivery: in vitro, in vivo and ex vivo study, Pharmaceutics 12 (3) (2020) 219.

[30] N. Meshginfar, et al., OPTIMIZATION OF THE PRODUCTION OF PROTEIN HYDROLYSATES FROM MEAT INDUSTRY BY PRODUCTS BY RESPONSE SURFACE METHODOLOGY, 2014.

[31] S. Kaveh, et al., Optimization of factors affecting the antioxidant activity of fenugreek seed's protein hydrolysate by response surface methodology, Iranian Journal of Nutrition Sciences & Food Technology 14 (1) (2019).

[32] L. Zhu, et al., Reducing, radical scavenging, and chelation properties of in vitro digests of alcalase-treated zein hydrolysate, J. Agric. Food Chem. 56 (8) (2008) 2714–2721.

[33] P. Sikorski, et al., Evidence for egg-box-compatible interactions in calcium– alginate gels from fiber X-ray diffraction, Biomacromolecules 8 (7) (2007) 2098–2103.

[34] J. Lee, D. Cha, H. Park, Survival of freeze-dried Lactobacillus bulgaricus KFRI 673 in chitosan-coated calcium alginate microparticles, J. Agric. Food Chem. 52 (24) (2004) 7300–7305.

[35] W. Krasaekoopt, S. Watcharapoka, Effect of addition of inulin and galactooligosaccharide on the survival of microencapsulated probiotics in alginate beads coated with chitosan in simulated digestive system, yogurt and fruit juice, LWT–Food Sci. Technol. 57 (2) (2014) 761–766.

[36] D. Bhopatkar, A. Anal, W. Stevens, Ionotropic alginate beads for controlled intestinal protein delivery: effect of chitosan and barium counter-ions on entrapment and release, J. Microencapsul. 22 (1) (2005) 91–100.

[37] H. Daemi, M. Barikani, Synthesis and characterization of calcium alginate nanoparticles, sodium homopolymannuronate salt and its calcium nanoparticles, Sci. Iran. 19 (6) (2012) 2023–2028.

[38] J.A. Araujo, et al., Composite films of thermoplastic starch and CaCl2 extracted from eggshells for extending food shelf-life, Polysaccharides 2 (3) (2021) 677–690.

[39] D. Lu, et al., Effect of enzymatic hydrolysis on the zinc binding capacity and in vitro gastrointestinal stability of peptides derived from pumpkin (Cucurbita pepo L.) seeds, Front. Nutr. 8 (2021) 647782.

[40] M.F. Queiroz, et al., Does the use of chitosan contribute to oxalate kidney stone formation? Mar. Drugs 13 (1) (2014) 141–158.

[41] M. Wang, et al., Preparation of pH-sensitive carboxymethyl cellulose/chitosan/alginate hydrogel beads with reticulated shell structure to deliver Bacillus subtilis natto, Int. J. Biol. Macromol. 192 (2021) 684–691.

[42] B. Cai, et al., Preparation, characterization and in vitro release study of drug-loaded sodium carboxy-methylcellulose/chitosan composite sponge, PLoS One 13 (10) (2018) e0206275.

[43] H. Gao, et al., Investigation of the thermo-mechanical properties of blend films based on hemicelluloses and cellulose, International Journal of Polymer Science (2018) 2018.

[44] G. da Silva Filipini, V.P. Romani, V.G. Martins, Biodegradable and active-intelligent films based on methylcellulose and jambolão (Syzygium cumini) skins extract for food packaging, Food Hydrocolloids 109 (2020) 106139.

[45] L. Motelica, et al., Biodegradable alginate films with ZnO nanoparticles and citronella essential oil—a novel antimicrobial structure, Pharmaceutics 13 (7) (2021) 1020.

[46] L.A. Caetano, A.J. Almeida, L.M. Gonçalves, Effect of experimental parameters on alginate/chitosan microparticles for BCG encapsulation, Mar. Drugs 14 (5) (2016) 90.

[47] Z. Zhang, et al., Protein encapsulation in alginate hydrogel beads: effect of pH on microgel stability, protein retention and protein release, Food Hydrocolloids 58 (2016) 308–315.

[48] P. Bacchin, et al., Surface pre-coating of talc particles by carboxyl methyl cellulose adsorption: study of adsorption and consequences on surface properties and settling rate, Colloids Surf. A Physicochem. Eng. Asp. 272 (3) (2006) 211–219.

[49] M. Yousefi, et al., Encapsulation of Heracleum persicum essential oil in chitosan nanoparticles and its application in yogurt, Front. Nutr. 10 (2023) 1130425.

[50] E. Joseph, G. Singhvi, Multifunctional nanocrystals for cancer therapy: a potential nanocarrier, Nanomaterials for drug delivery and therapy (2019) 91–116.

[51] A.J. Shnoudeh, et al., Synthesis, characterization, and applications of metal nanoparticles, in: Biomaterials and Bionanotechnology, Elsevier, 2019, pp. 527–612.

[52] F. Maestrelli, et al., Development of enteric-coated calcium pectinate microspheres intended for colonic drug delivery, Eur. J. Pharm. Biopharm. 69 (2) (2008) 508–518.

[53] X. Li, et al., Preparation of alginate coated chitosan microparticles for vaccine delivery, BMC Biotechnol. 8 (1) (2008) 1–11.

[54] M. Yao, D.J. McClements, H. Xiao, Improving oral bioavailability of nutraceuticals by engineered nanoparticle-based delivery systems, Curr. Opin. Food Sci. 2 (2015) 14–19.

[55] Y. Chen, et al., Development, characterization, stability and bioaccessibility improvement of 7, 8-dihydroxyflavone loaded zein/sophorolipid/polysaccharide ternary nanoparticles: comparison of sodium alginate and sodium carboxymethyl cellulose, Foods 10 (11) (2021) 2629.

[56] S. Rebolleda, et al., Formulation and characterisation of wheat bran oil-in-water nanoemulsions, Food Chem. 167 (2015) 16–23.

[57] S. Taymouri, J. Varshosaz, Effect of different types of surfactants on the physical properties and stability of carvedilol nano-niosomes, Adv. Biomed. Res. 5 (2016).

[58] M.t.M. Alsmadi, et al., Development, in vitro characterization, and in vivo toxicity evaluation of chitosan-alginate nanoporous carriers loaded with cisplatin for lung cancer treatment, AAPS PharmSciTech 21 (2020) 1–12.

[59] J. Lei, J.-H. Kim, Y.S. Jeon, Preparation and Properties of Alginate/polyaspartate Composite Hydrogels, vol. 16, Macromolecular Research, 2008, pp. 45–50.

[60] F.T. Dolatabadi, F.E. Vasheghani, H. Mirzadeh, Swelling Behaviour of Alginate-N, Ocarboxymethyl Chitosan Gel Beads Coated by Chitosan, 2006.

[61] X. Wang, et al., Fabrication and characterization of zein-tea polyphenols-pectin ternary complex nanoparticles as an effective hyperoside delivery system: formation mechanism, physicochemical stability, and in vitro release property, Food Chem. 364 (2021) 130335.

[62] D. Lin, et al., Effect of structuring emulsion gels by whey or soy protein isolate on the structure, mechanical properties, and in-vitro digestion of alginate-based emulsion gel beads, Food Hydrocolloids 110 (2021) 106165.

[63] R. Sun, Q. Xia, In vitro digestion behavior of (W1/O/W2) double emulsions incorporated in alginate hydrogel beads: microstructure, lipolysis, and release, Food Hydrocolloids 107 (2020) 105950.

[64] G. Pasparakis, N. Bouropoulos, Swelling studies and in vitro release of verapamil from calcium alginate and calcium alginate–chitosan beads, Int. J. Pharm. 323 (1–2) (2006) 34–42.

[65] L.G. Gómez-Mascaraque, et al., Nano-and microstructural evolution of alginate beads in simulated gastrointestinal fluids. Impact of M/G ratio, molecular weight and pH, Carbohydr. Polym. 223 (2019) 115121.

[66] S.J. Buwalda, et al., Hydrogels in a historical perspective: from simple networks to smart materials, J. Contr. Release 190 (2014) 254–273.

[67] Y. Hu, et al., A double-layer hydrogel based on alginate-carboxymethyl cellulose and synthetic polymer as sustained drug delivery system, Sci. Rep. 11 (1) (2021) 9142.

[68] Y. Hu, et al., Construction and evaluation of the hydroxypropyl methyl cellulose-sodium alginate composite hydrogel system for sustained drug release, J. Polym. Res. 25 (2018) 1–12.

[69] M.F. Bósquez-Cáceres, et al., Chitosan-carboxymethylcellulose hydrogels as electrolytes for zinc–air batteries: an approach to the transition towards renewable energy storage devices, Batteries 8 (12) (2022) 265.

[70] A.M. Nikoo, et al., Electrospray-assisted encapsulation of caffeine in alginate microhydrogels, Int. J. Biol. Macromol. 116 (2018) 208–216.

[71] K. Mulia, A.C. Singarimbun, E.A. Krisanti, Optimization of chitosan–alginate microparticles for delivery of mangostins to the colon area using box–behnken experimental design, Int. J. Mol. Sci. 21 (3) (2020) 873.

[72] C. Zhang, et al., Nano-in-micro alginate/chitosan hydrogel via electrospray technology for orally curcumin delivery to effectively alleviate ulcerative colitis, Mater. Des. 221 (2022) 110894.

[73] G. Coppi, et al., Chitosan-alginate microparticles as a protein carrier, Drug Dev. Ind. Pharm. 27 (5) (2001) 393–400.

[74] A. Belščak-Cvitanović, et al., Encapsulation of polyphenolic antioxidants from medicinal plant extracts in alginate–chitosan system enhanced with ascorbic acid by electrostatic extrusion, Food Res. Int. 44 (4) (2011) 1094–1101.

[75] S. Reyhani Poul, S. Yeganeh, Physicochemical and antioxidant properties of chitosan-coated nanoliposome loaded with bioactive peptides produced from shrimp wastes hydrolysis, Iran. J. Fish. Sci. 21 (4) (2022) 987–1003.

[76] A. Sankar, et al., Antioxidant activity of chitosan nanoparticles with chlorhexidine-an in vitro study, Journal of Population Therapeutics and Clinical Pharmacology 30 (14) (2023) 33–40.